Color Doppler Imaging of Intracranial Vessels in the Neonate

Wilson S. Wong, Jay S. Tsuruda, Ricardo L. Liberman, Ana Chirino, John F. Vogt and Ernesto Gangitano

AJNR Am J Neuroradiol 1989, 10 (2) 425-430
http://www.ajnr.org/content/10/2/425

Color Doppler Imaging of Intracranial Vessels in the Neonate

Wilson S. Wong[1]
Jay S. Tsuruda[1,2]
Ricardo L. Liberman[3]
Ana Chirino[1]
John F. Vogt[3]
Ernesto Gangitano[3]

This study was performed to examine the effectiveness of color Doppler imaging (CDI) in demonstrating the neonatal intracranial vessels and altered intracranial flow patterns and to determine the optimal approach in imaging the intracranial vasculature. The study was conducted in two parts. First, 14 neonates were examined with CDI by using a standard approach through the anterior fontanel. Whenever possible, views through the posterior fontanel and the temporal bone were obtained also. The anterior cerebral, M1 segment of the middle cerebral, distal internal carotid, and basilar arteries were demonstrated consistently. Portions of the vertebral, distal middle cerebral, and posterior cerebral arteries were frequently visualized. In the second part of the study, we examined 10 neonates who had undergone extracorporeal membrane oxygenation. In this group of patients, CDI was able to demonstrate occlusion of the right internal carotid artery and the reversal of flow through the ipsilateral A1 segment. Increased flow on the contralateral side and in the basilar artery was observed in several patients.

The anterior fontanel approach was shown to be the most useful in identifying most of the major intracranial arteries and veins with CDI. In addition, the body weights and gestational ages of the neonates were found to significantly influence the success rate in visualizing the intracranial vasculature.

Color Doppler imaging (CDI) is a recent innovation in which color-encoded flow data of a vascular structure are displayed simultaneously on a real-time gray-scale B-mode image [1–3]. In the field of echocardiography, CDI has proved to be effective in the study of normal cardiac anatomy [4], valvular disease [5], cardiomyopathies [6], and congenital heart disease [7]. Extracardiac analysis of blood flow has also been described for evaluation of arterial pseudoaneurysms [8, 9], intratumoral blood flow [10], and abdominal organ perfusion [11]. Its potential application in noninvasive neurovascular imaging has been recognized, and preliminary results with carotid disease [11], intracranial arteriovenous malformations [12], and neonatal intracranial vascular analysis [11] have been reported.

Neonatal cranial sonography has been used mainly in screening premature neonates for intracranial hemorrhage. Additional studies with duplex Doppler imaging have been shown to be helpful in measuring cerebral blood flow and velocity [13–19]. Extracorporeal membrane oxygenation (ECMO) is gaining widespread acceptance as a method of treatment for severe respiratory insufficiency in neonates unresponsive to conventional respiratory therapy [20–23]. This procedure is associated with significant alterations of intracranial hemodynamics [24]. Hence, it would be of great clinical interest to be able to study the intracranial flow patterns of this group of patients noninvasively. Although high-resolution sonography has at times been able to image intracranial vessels in neonates, the ability to demonstrate flow by CDI greatly improves the visualization of these vessels. The objectives of this study were to examine the effectiveness of CDI in demonstrating the neonatal intracranial vessels and altered flow patterns and to determine the optimal approach in imaging the intracranial vasculature.

This article appears in the March/April 1989 issue of *AJNR* and the May 1989 issue of *AJR*.

Received April 22, 1988; accepted after revision July 25, 1988.

Presented at the annual meeting of the American Society of Neuroradiology, Chicago, May 1988.

[1] Department of Radiology, Huntington Memorial Hospital, 100 Congress St., Pasadena, CA 91105. Address reprint requests to W. S. Wong.

[2] Huntington Medical Research Institutes, Pasadena, CA 91105.

[3] Department of Neonatology, Huntington Memorial Hospital, Pasadena, CA 91105.

***AJNR* 10:425–430, March/April 1989**
0195–6108/89/1002–0425

Materials and Methods

Patient Population

The patient population consisted of 24 neonates with a mean gestational age of 34 weeks (range, 26–43 weeks). The average weight of the patients was 2176 g (range, 590–4400 g). Neonatal cranial sonography was requested for 11 patients to rule out intracranial hemorrhage and for 10 patients as a routine part of the ECMO procedure. The indications for the remaining three patients were spina bifida, hydrocephalus, and periventricular leukomalacia. In three ECMO patients, serial studies were performed, bringing the total number of studies to 29.

Sonographic Technique

An Acuson 128 color Doppler phase-array scanner* was used for all cases. The examination was performed at the bedside in the neonatal intensive care unit. A conventional B-mode examination was performed with a 5-MHz sector transducer (S519) and was followed by CDI with a 5-MHz linear-array (L538) transducer. The spatial peak temporal average of the equipment estimated in situ was maintained at all times below 94 mW/cm^2. With CDI, the ultrasound signal is detected and analyzed in real time for changes in echo amplitude, frequency, and phase shifts. These changes provide information on the presence and direction of motion relative to the transducer and the relative velocities compared with stationary objects [11]. The results are displayed as a composite image consisting of a background B-mode image with encoded flow information displayed in color. Depending on the direction of flow with respect to the transducer, the data displayed are either red or blue. In this study, for the majority of the images, red was assigned as flow toward and blue as flow away from the transducer. On rare occasions, this was arbitrarily reversed so that venous structures were shown in blue while arterial segments were red. Flow velocity is indicated as the degree of saturation of color, with more saturation indicating higher velocities. In regions of very high velocity and/or turbulent (random) flow, increased color saturation is present and the vessel becomes white. The same machine was equipped with duplex Doppler scanning, which was useful in measuring flow velocity and in distinguishing between arterial and venous flow by spectral analysis after identifying the vessel by CDI. All images were recorded on videotape for later analysis.

Scanning Approaches

Our scanning protocol consisted of three different approaches: the anterior fontanel, the posterior fontanel, and the squamous portion of the temporal bone. The anterior fontanel approach used conventional coronal views obtained from the anteriormost to the posteriormost aspect of the brain (Fig. 1). This was followed by side-to-side parasagittal sections (Fig. 2). All patients were examined with this approach. With the posterior fontanel approach, the transducer was oriented in the axial plane (Fig. 3). Fifteen patients were studied by this approach. For the temporal approach [15], the transducer was also oriented in the axial plane. By placing the transducer 0.5–1 cm anterior to the external auditory canal and superior to the zygomatic process, the ultrasound beam passes through the relatively thin squamous portion of the temporal bone or the anterolateral fontanel, which may be open in neonates (Fig. 4). In the majority of cases, only one side (i.e., left or right temporal view) was obtained, since the depth of penetration of the transducer was adequate to visualize the contralateral vessels. We were able to evaluate 16 patients by the temporal approach. In a minority of patients, either the temporal or the posterior fontanel approach or neither was used when the pa-

* Acuson, Mountain View, CA.

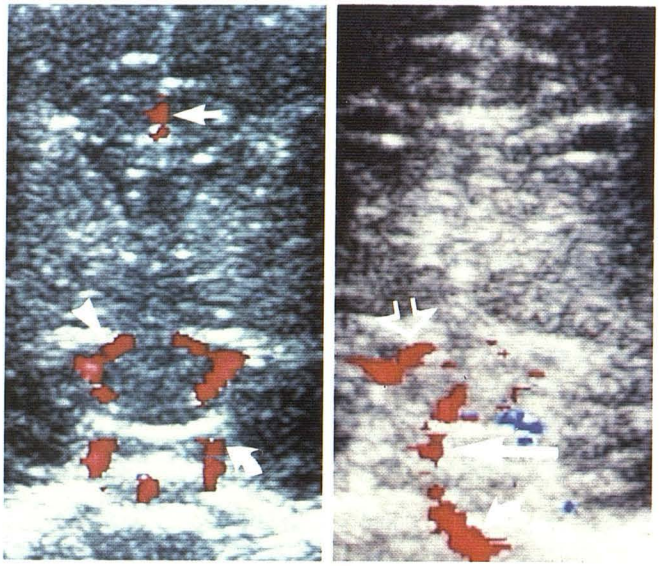

Fig. 1.—Coronal views via anterior fontanel approach.
***A*, Scan through anterior portion of circle of Willis: right A1 segment (*arrowhead*), left distal internal carotid artery (*curved arrow*), and pericallosal artery (*straight arrow*).**
***B*, Scan slightly posterior to *A* shows basilar artery (*solid straight arrow*), left vertebral artery (*curved arrow*), and portion of right posterior cerebral artery (*open arrow*). Right vertebral artery (not shown) was also seen, but not in the same imaging plane.**

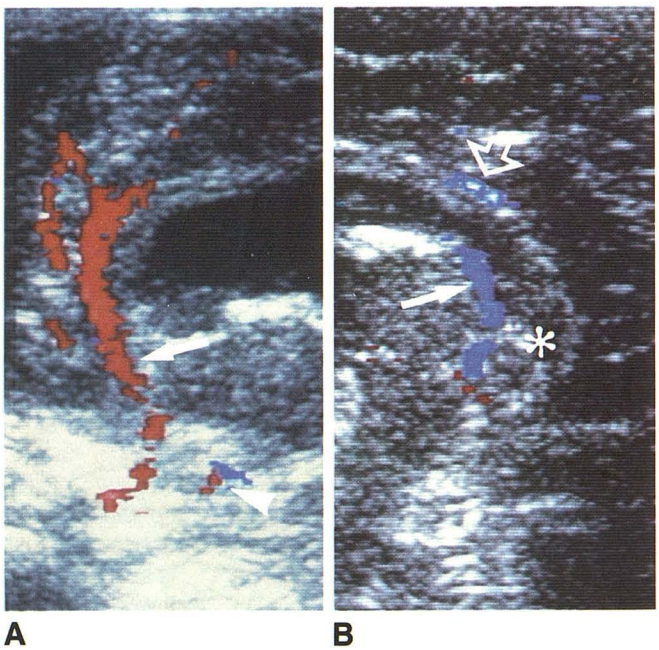

Fig. 2.—Sagittal views through anterior fontanel.
***A*, Anterior midline sagittal scan shows pericallosal artery (*arrow*) and its branches and distal portion of basilar artery (*arrowhead*). Note dilated lateral ventricle.**
***B*, Posterior midline sagittal scan shows internal cerebral vein (*solid arrow*) and inferior sagittal sinus (*open arrow*). *Asterisk* indicates splenium of corpus callosum.**

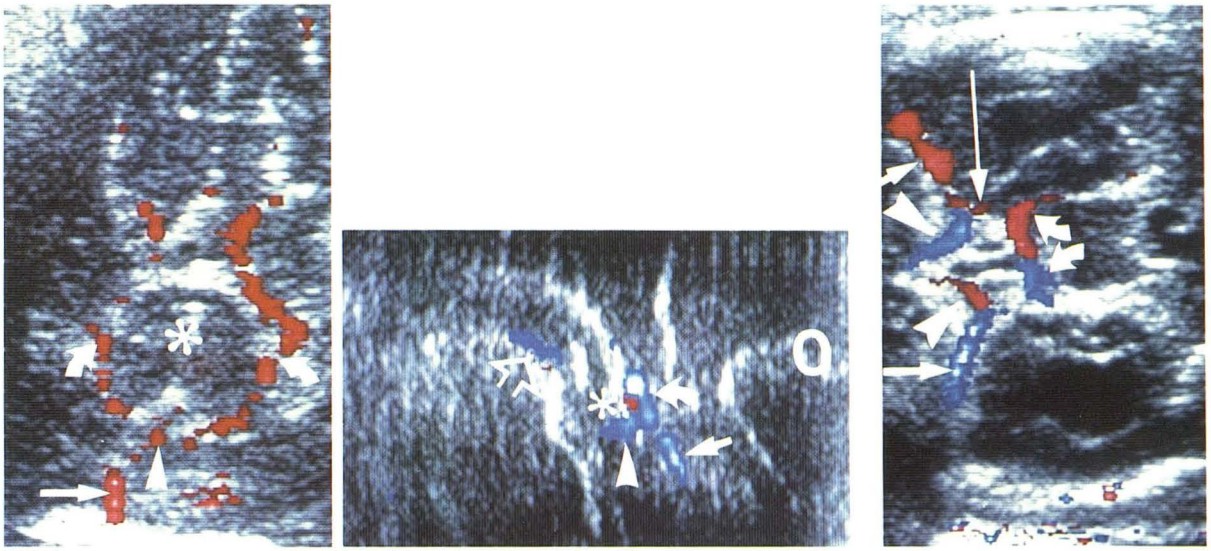

Fig. 3.—Posterior fontanel approach.

***A*, Axial scan shows posterior cerebral arteries (*curved arrows*) surrounding brainstem (*asterisk*), right internal carotid artery (*straight arrow*), and region of distal end of basilar artery (*arrowhead*).**

***B*, Midsagittal view shows vein of Galen (*arrowhead*), straight sinus (*straight arrow*), inferior sagittal sinus (*curved arrow*), and internal cerebral vein (*open arrow*). Splenium of corpus callosum (*asterisk*) is an important landmark. O indicates occipital region. (Note reversal of color assignment so that venous structures are blue.)**

Fig. 4.—Temporal approach. Transaxial scan through left temporal bone shows circle of Willis: A1 segment of anterior cerebral arteries (left side, blue; right side, red) (*arrowheads*); M1 segment of middle cerebral arteries (left side, red; right side, blue) (*short straight arrows*); posterior cerebral arteries (left side, red; right side, blue) (*curved arrows*); and left posterior communicating artery (*long straight arrow*).

tient's life-support system prevented adequate access to these areas. In every case, a systematic attempt was made to demonstrate each of the vessels being studied. All examinations were performed by the same technologist and radiologist. The average time to perform a complete study was 15–20 min.

Technical Considerations

Proper adjustment of the velocity scale to match the flow velocity of the vessel was found to be one of the critical factors for the success of the study. A change in the velocity scale directly reflected a change in the pulse repetition frequency or the sampling rate of the scanner. Setting the velocity scale to a high value makes the scanner less sensitive to slow flow within structures such as dural sinuses and internal cerebral veins. Conversely, with the velocity scale set to a low value, high-velocity flow may lead to excessive frequency shift, resulting in aliasing [2, 4], although this was not a serious problem in our patient population.

As with all Doppler examinations, the angle between the direction of flow and the ultrasound beam was an important factor, since a more parallel orientation will enhance color flow visualization of vessels [4, 25]. For example, the coronal view with the anterior fontanel approach demonstrates the M1 segment of the middle cerebral artery poorly. This is due to a nearly perpendicular angle between the direction of flow and the ultrasound beam. By using the temporal approach, the Doppler beam is nearly parallel to flow and the percent visualization is greatly improved.

Because the study is performed in real time, the transducer can be manipulated to optimize the Doppler angle. At the same time, maneuvering the transducer along the course of a tortuous vessel aids in the evaluation of vascular segments. With this method, a more complete appreciation of important structures such as the circle of Willis can be obtained, since only a small portion of this vascular ring may be seen at any given moment. Its relationship to other important, stationary structures, such as the midbrain and third ventricle, becomes apparent. The color shift from either red or blue based on flow direction aids in identifying a particular vessel and helps to define the contour of small branch vessels such as the distal anterior cerebral branches (Fig. 2A).

Data Analysis

The video recordings were reviewed by two radiologists for the following arteries: anterior cerebral (A1 segments and segments distal to the anterior communicating artery, consisting of the pericallosal artery and its branches), middle cerebral (M1 segments and distal branches including M2 and/or M3 segments), internal carotid, posterior cerebral, basilar, and vertebral. Because the A1 segments, M1 segments, distal middle cerebral branches, internal carotid, posterior cerebral, and vertebrals are paired structures, a numerical score of 0, 1, or 2 was assigned to each paired artery depending on whether none, one, or two of the arteries were seen. This tabulation was performed for each of the three approaches. Distinguishing the two distal anterior cerebral artery segments was not possible because of the closeness of these vessels; therefore, the expected score was 1. The percentage of each artery visualized was computed as follows: percent visualized = total of the numerical score/total number of expected vessels $\times$ 100. Although the posterior communicating artery is an important component of the circle of Willis, because of its smaller caliber, it was demonstrated infrequently and was not included as part of the tabulation.

The venous structures, which included the internal cerebral veins, vein of Galen, straight sinus, and superior sagittal/inferior sagittal sinus complex, were studied in a similar fashion. A numerical score of 1 or 0 was assigned to each vessel depending on whether or not it was seen. Like the distal anterior cerebral arterial segments, it was

not possible to distinguish between the right and left internal cerebral veins.

Statistical Analysis

To determine if the patient's gestational age influenced the percent vessel visualization, the entire study group of 24 patients was arbitrarily divided into two subgroups: ≤35 weeks (12 patients) and >35 weeks (12 patients). Comparison was made for each of the three approaches by using a Student t test for paired observations. A value of $p < .05$ was considered significant. A similar analysis was performed on the study group as a function of body weight by dividing the patients into two subgroups: ≤2000 g (12 patients) or >2000 g (12 patients).

ECMO Patients

The most common intracranial complication in ECMO patients is intracranial hemorrhage [26, 27]. Serial real-time neonatal cranial sonography was performed mainly to check for development of this problem. In this subgroup of patients, CDI was also used to examine for collateral flow patterns such as flow reversal and change in vascular caliber. In three ECMO patients, CDI was performed serially before and immediately after the ECMO procedure.

Results

Anterior Fontanel Approach

The anterior fontanel approach was the most readily accessible view and yielded the best anatomic detail because of its relatively large size, which provides a good acoustic window. By using a combination of coronal (Fig. 1) and sagittal (Fig. 2) scans, most of the major intracranial vessels could be identified consistently, including the anterior cerebral arteries (A1 and distal segments), internal carotid arteries, and basilar artery. The M1 segments of the middle cerebral artery were demonstrated less well by this approach because the direction of blood flow through this arterial segment is nearly perpendicular to the Doppler beam. With the midsagittal view, the internal cerebral vein was demonstrated relatively well (Fig. 2B) and the vein of Galen was imaged infrequently.

Posterior Fontanel Approach

The posterior fontanel approach was more limited in its field of view because of the comparatively smaller size of this fontanel. An oblique axial approach obtained by angulating the beam toward the midbrain was most effective in defining the arteries of the posterior cerebrum, including the interpeduncular, perimesencephalic, quadrigeminal, and distal segments of the posterior cerebral arteries (Fig. 3A). The distalmost portion of the basilar and internal carotid arteries were visualized inconsistently. If an optimal-flow Doppler beam angle was obtained, flow in the vein of Galen and the straight sinus could be seen (Fig. 3B).

Temporal Approach

The temporal approach through the thin squamous portion of the temporal bone and/or anterolateral fontanel provided detailed images of the midbrain and the vessels forming the circle of Willis, especially the proximal segments of the anterior and middle cerebral arteries (Fig. 4). Compared with the anterior fontanel approach, the middle cerebral arteries were demonstrated better because of the more favorable Doppler angle [15].

Percent Visualization

The percent visualization of both the arteries and veins with respect to the approaches are summarized in Table 1. Data analysis of percent vessel visualization with respect to body weight (≤2000 g or >2000 g) and gestational age (≤35 weeks or >35 weeks) appears in Table 2. For body weight statistical differences in the overall percent vascular visualization was noted in all three approaches, with better demonstration of vessels in the smaller body weight (≤2000 g) subgroup. Gestational age had less effect on percent vessel visualization, except for the posterior fontanel approach, which had a higher percent visualization in the ≤35-week subgroup.

ECMO Patients

After right common carotid ligation, reversal of flow direction in the A1 segment of the right anterior cerebral artery was seen consistently in all 10 ECMO patients. This finding was well demonstrated with the anterior and temporal approaches (Fig. 5). Flow within the right middle cerebral artery could be demonstrated also. On occasion, retrograde flow in the distal right internal carotid artery was seen. In a limited number of patients, collateral vessels of the circle of Willis, including the distal portion of the basilar artery, were anecdotally noted to have a greater than expected degree of

TABLE 1: Percent Visualization of Arteries and Veins vs Approach: All Patients

Vessel: Branch	% Visualization via:		
	Anterior Fontanel	Posterior Fontanel	Temporal
Artery:			
Anterior cerebral:			
A1 segments	71	0	9
Distal segments	90	0	0
Middle cerebral:			
M1 segments	44	0	95
Distal segments	23	0	13
Posterior cerebral	66	62	68
Basilar	97	12	30
Vertebral	45	0	0
Internal carotids	82	12	15
Vein:			
Internal cerebral	74	6	0
Vein of Galen	35	47	32
Straight sinus	10	12	0
Superior and/or inferior sagittal sinus	18	6	0

TABLE 2: Percent Arterial and Venous Visualization vs Approach: Effects of Body Weight and Gestational Age

Variable	% Visualization via:		
	Anterior Fontanel	Posterior Fontanel	Temporal
Body weight:			
≤2000 g ($n = 12$)	61	22	41
>2000 g ($n = 12$)	49	5	23
Significance (p)	.036	.011	.043
Gestational age:			
≤35 weeks ($n = 12$)	52	19	28
>35 weeks ($n = 12$)	55	6	25
Significance (p)	NS	.014	NS

Note.—NS = not significant. Significance was determined from paired t test.

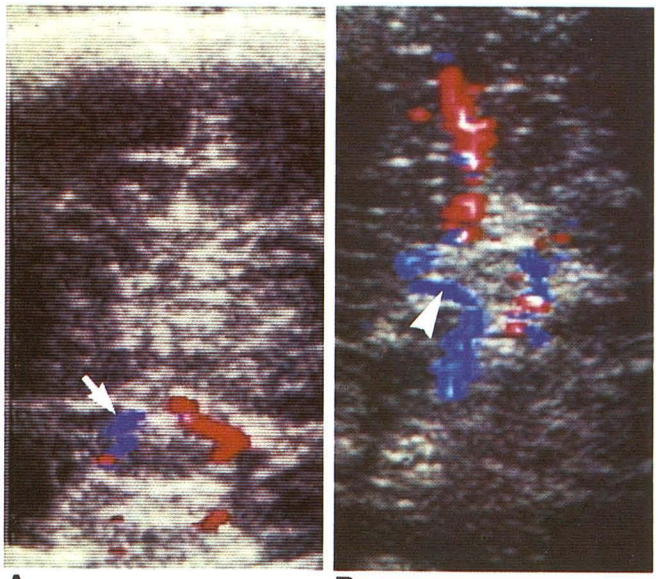

Fig. 5.—Patient who had undergone extracorporeal membrane oxygenation procedure with ligation of right common carotid artery.

***A*, Coronal view through anterior fontanel shows reversal of flow (blue color indicates flow is away from transducer) in A1 segment (*arrow*) of right anterior cerebral artery.**

***B*, Transaxial view through left temporal bone shows flow pattern in right A1 segment (*arrowhead*) similar to that in *A*. Compare this pattern with that in Fig. 4.**

caliber and flow when compared with non-ECMO patients. However, because of the limited access to these critically ill neonates, no attempt was made to further quantify this observation by volumetric flow analysis with pulsed Doppler.

Discussion

In this preliminary study, we have been able to show the effectiveness of CDI in visualizing neonatal intracranial vessels. In most patients, major intracranial arteries and veins could be identified in a high percentage of cases with a high degree of confidence. In addition, the study is noninvasive and rapid and can be performed in the neonatal intensive care unit or nursery on critically ill patients without disturbing life-support systems. Performing this type of examination does require technical skill and the results are highly operator-dependent. We noticed that the ease of obtaining adequate images and the length of time of the examination improved significantly with experience.

From the data presented in Table 1, specific approaches were found to be more useful in demonstrating certain vessels; these are summarized in Table 3. The readily accessible anterior fontanel approach was the most helpful in identifying most of the major intracranial arteries and veins. Of particular importance was its value in visualizing the distal branches of the anterior cerebral artery, as well as the basilar, vertebral, and internal carotid arteries. The midsagittal view from this approach yielded the most information in demonstrating the major intracranial veins and dural sinuses. The temporal approach was the second most useful approach, especially in evaluating the A1 and M1 segments of the anterior and middle cerebral arteries, respectively, due to optimization of the Doppler angle when compared with the anterior fontanel approach (Fig. 4).

TABLE 3: Best Approaches in Imaging the Arteries

Artery	Best Approach
Anterior cerebral:	
A1 segments	Anterior fontanel (coronal) or temporal (axial)
Distal segments	Anterior fontanel (sagittal)
Middle cerebral:	
M1 segments	Temporal (axial)
Distal segments	Anterior fontanel (sagittal)
Posterior cerebral	Posterior fontanel (axial)
Basilar	Anterior fontanel (coronal or sagittal)
Vertebral	Anterior fontanel (coronal)
Internal carotids	Anterior fontanel (coronal)

Finally, on the basis of total percent vessel visualization, the posterior fontanel approach was the least useful. However, in some patients, the posterior fontanel view was excellent in studying the distal branches of the posterior cerebral artery (Fig. 3A), since the direction of flow was directly toward the ultrasound beam. Because the vein of Galen has a similar flow direction, it could be seen in approximately half the patients. Less success was noted in detecting the straight sinus, presumably due to its more inferior flow direction away from the posterior fontanel (Fig. 3B).

The patient population may also affect the overall success of CDI in detecting both arterial and venous structures. From the data summarized in Table 2, a higher, statistically significant percent vessel visualization was obtained with all three approaches in patients weighing 2000 g or less, reflecting the presence of larger fontanel size and smaller brain volume, which allowed better ultrasound beam penetration. In addition, this group included several small-for-gestational-age neonates. In this subgroup, higher intracranial arterial flow velocities have been recorded by standard Doppler analysis [19] and presumably would improve visualization by CDI. Unfortunately, because of the small number of neonates in our study population who were small for gestational age, it was not possible to statistically compare this subgroup with neonates who had appropriate weight for gestational age.

In addition to body weight, gestational age may influence the percent vascular visualization, as outlined in Table 2. After arbitrarily dividing the study population into two subgroups ($\leq$35 weeks and >35 weeks), no significant differences were noted when they were compared for either the anterior fontanel or temporal approach. However, a statistically greater percent visualization was noted in the $\leq$35-week subgroup when CDI was performed through the posterior fontanel. This difference may be explained by the generally smaller size of this fontanel, which may be closed in term neonates [28].

In ECMO patients, CDI appears to be a sensitive indicator of altered flow patterns. In this procedure, both the right common carotid artery and jugular vein are cannulated with large-caliber catheters. The oxygen-poor blood from the right atrium is drained by gravity into a reservoir via the cannula in the right jugular vein. The blood is then pumped into a thin membrane, which is exposed to a controlled mixture of oxygen, carbon dioxide, and room air. The oxygenated blood is then pumped back to the patient's aortic arch via the catheter in the right carotid artery. These patients provide a unique opportunity to study changes in intracranial flow patterns in vivo, since irreversible ligation of both the common right

carotid artery and jugular vein is performed for the bypass procedure. In addition, other noninvasive studies, including IV digital subtraction angiography and xenon cerebral blood flow determinations, have shown that perfusion of the right cerebral hemisphere by collateral flow is present [23]. This collateral flow pattern, seen as reversal of flow within the right A1 segment of the anterior cerebral artery and antegrade filling of the right M1 segment of the middle cerebral artery, can be demonstrated by CDI. As expected, the posterior communicating arteries would also be important collaterals. Conceptually, the temporal approach would be the optimal view to delineate these vessels. However, because of the nearly perpendicular Doppler beam/flow angle, the posterior communicating arteries were visualized inconsistently (Fig. 4). Reversal of flow within the distal segment of the right internal carotid artery was also seen, which may be an indirect indicator of retrograde supply to other important arteries, such as the right ophthalmic and right external carotid. In patients who had serial studies before and after the ECMO bypass procedure, a qualitative increase in the caliber and pulsation of the intracranial arteries was detected on ECMO, presumably reflecting the known decrease in cerebral vascular resistance and increase in cerebral blood flow as demonstrated by Doppler waveform analysis [24].

CDI may have other potential applications in neurovascular imaging. CDI may assist in the more precise placement of the sample volume for quantitative Doppler spectral analysis and aid in measuring the Doppler angle, thus improving the accuracy of velocity measurements. This technique may also help in diagnosing major intracranial vascular anomalies such as vein of Galen aneurysms, as well as providing intraoperative guidance. We also have begun to apply CDI in evaluating arterioocclusive diseases such as vasculitis and moyamoya. Before performing an ECMO bypass, documenting the lack of collaterals such as an atretic A1 segment may have a role in predicting acute complications such as cerebral infarction and later neurodevelopmental delay. This should be an area of further investigation.

On the other hand, CDI requires considerable operator skill and experience. Care must be taken to detect slow venous flow. In most cases, the major intracranial venous and dural sinuses will not be evaluated adequately, and therefore its use in documenting dural sinus thrombosis may be limited.

In summary, our results show that CDI has a role in the noninvasive evaluation of neonatal intracranial vessels. This technique can be applied readily during the standard B-mode sonographic examination and can provide qualitative information on normal and abnormal flow patterns. With further refinement in the scanner technology, such as the use of sector instead of linear transducers, an improvement in the overall accuracy of this technique is anticipated.

ACKNOWLEDGMENTS

We thank Kathy Cislo and Tom Jedrzejewicz for help in photographing the illustrations and Fred A. Lee and Richard A. Yadley for reviewing the manuscript.

REFERENCES

1. Merritt CRB. Doppler blood flow imaging: integrating flow with tissue data. *Diagn Imaging* **1986**;8:146–155
2. Omoto R, Kasai C. Physics and instrumentation of Doppler color flow mapping. *Echocardiography* **1987**;4:467–483
3. Taylor KJW. Going to the depths with duplex Doppler ultrasound. *Diagn Imaging* **1987**;9:106–116
4. Harrison MR, Smith MD, Grayburn PA, Kwan OL, DeMaria AN. Normal blood flow patterns by color Doppler flow imaging. *Echocardiography* **1987**;4:485–493
5. Perry GJ, Nanda NC. Recent advances in color flow Doppler evaluation of valvular regurgitation. *Echocardiography* **1987**;4:503–513
6. Mills TJ, Seward JB, Khandheria BK, Klein AL, Oh JK, Tajik AJ. Color flow imaging in cardiomyopathies: observations and implications. *Echocardiography* **1987**;4:527–534
7. Ritter SB. Application of color flow mapping in the assessment and the evaluation of congenital heart disease. *Echocardiography* **1987**;4:543–556
8. Mitchell DG, Needleman L, Bezzi M, et al. Femoral artery pseudoaneurysm: diagnosis with conventional duplex and color Doppler US. *Radiology* **1987**;165:687–690
9. Wong WS. Case report. Detection of a pinhole opening of a false aneurysm by color flow Doppler. *Echocardiography* **1987**;4:569–571
10. Shinamoto K, Sakuma S, Ishigaki T, Makino N. Intratumoral blood flow: evaluation with color Doppler echography. *Radiology* **1987**;165:683–685
11. Merritt CRB. Doppler color flow imaging. *JCU* **1987**;15:591–597
12. Black KL, Rubin JM, Chandler WF, McGillicuddy JE. Intraoperative color-flow Doppler imaging of AVM's and aneurysms. *J Neurosurg* **1988**;68:635–640
13. Bada HS, Hajjar W, Chua C, Sumner DS. Noninvasive diagnosis of neonatal asphyxia and intraventricular hemorrhage by Doppler ultrasound. *J Pediatr* **1979**;95:775–779
14. Miles RD, Menke JA, Bashiru M, Colliver JA. Relationships of five Doppler measures with flow in an in vitro model and clinical findings in newborn infants. *J Ultrasound Med* **1987**;6:597–599
15. Raju TNK, Zikos E. Regional cerebral blood velocity in infants. A real-time transcranial and fontanellar pulsed Doppler study. *J Ultrasound Med* **1987**;6:497–507
16. van Bel F, van de Bor M, Buis-Liem TN, Stijnen T, Baan J, Ruys JH. The relation between left-to-right shunt due to patent ductus arteriosis and cerebral blood flow velocity in preterm infants. *J Cardiovasc Ultrasonogr* **1987**;6:19–25
17. van Bel F, van de Bor M, Stijnen T, Baan J, Ruys JH. Aetiological role of cerebral blood-flow alterations in development and extension of periintraventricular haemorrhage. *Dev Med Child Neurol* **1987**;29:601–614
18. van Bel F, van de Bor M, Stijnen T, Baan J, Ruys JH. Cerebral blood flow velocity pattern in healthy and asphyxiated newborns: a controlled study. *Eur J Pediatr* **1987**;146:461–467
19. van Bel F, van de Bor M, Stijnen T, Ruys JH. Decreased cerebrovascular resistance in small for gestational age infants. *Eur J Obstet Gynecol Reprod Biol* **1986**;23:137–144
20. Bartlett RH, Gazzaniga AB, Toomasian J, Corwin AG, Roloff D, Rucker R. Extracorporeal membrane oxygenation (ECMO) in neonatal respiratory failure. *Ann Surg* **1986**;204:236–245
21. Bartlett RH, Roloff DW, Cornell RG, Andrews AF, Dillion PW, Zwischenberger JF. Extracorporeal circulation in neonatal respiratory failure: a prospective randomized study. *Pediatrics* **1985**;76:479–487
22. Spahr RC. Extracorporeal membrane oxygenation in acute respiratory insufficiency in neonates: a review of the literature. *J Extra-Corporeal Technol* **1985**;17:111–116
23. Voorhies TM, Tardo CL, Starrett AL, et al. Evaluation of the cerebral circulation in neonates following extracorporeal membrane oxygenation (abstr). *Ann Neurol* **1985**;18:380
24. Taylor GA, Catena LM, Garin DB, Miller MK, Short BL. Intracranial flow patterns in infants undergoing extracorporeal membrane oxygenation: preliminary observations with Doppler US. *Radiology* **1987**;165:671–674
25. DeMaria AN, Spain MG, Garrahy P, Grayburn PA, Kwan OL, Smith MD. Considerations in the quantitation of color Doppler flow imaging. *Echocardiography* **1987**;4:495–501
26. Taylor GA, Fitz CR, Miller MK, Garin DB, Catena LM, Short BL. Intracranial abnormalities in infants treated with extracorporeal membrane oxygenation: Imaging with US and CT. *Radiology* **1987**;165:675–678
27. Taylor GA, Glass P, Fitz CR, Miller MK. Neurologic status in infants treated with extracorporeal membrane oxygenation: correlation of imaging findings with developmental outcome. *Radiology* **1987**;165:679–682
28. Harwood-Nash DC, Fitz CR. *Neuroradiology in infants and children*, vol. 1. St. Louis: Mosby, **1976**:41–44